Nuclear Engineering and Technology 50 (2018) 654–664

Contents lists available at ScienceDirect

Nuclear Engineering and Technology

journal homepage: www.elsevier.com/locate/net

Original Article

Self-pressurization analysis of the natural circulation integral nuclear reactor using a new dynamic model

Ali Farsoon Pilehvar [a], Mohammad Hossein Esteki [b, *], Afshin Hedayat [c], Gholam Reza Ansarifar [a]

[a] Department of Nuclear Engineering, Faculty of Advanced Sciences & Technologies, University of Isfahan, Hezarjarib Avenue, 81746-73441 Isfahan, Iran
[b] Department of Biomedical Engineering, Faculty of Engineering & Technologies, University of Isfahan, Hezarjarib Avenue, 81746-73441 Isfahan, Iran
[c] Reactor and Nuclear Safety School, Nuclear Science and Technology Research Institute (NSTRI), End of North Karegar Street, 14399-51113, Tehran, Iran

ARTICLE INFO

Article history:
Received 13 September 2017
Received in revised form
18 February 2018
Accepted 13 March 2018
Available online 12 April 2018

Keywords:
Condensation Power
Flashing Phenomenon
Natural Circulation
Self-Pressurization
Small Modular Reactor

ABSTRACT

Self-pressurization analysis of the natural circulation integral nuclear reactor through a new dynamic model is studied. Unlike conventional pressurized water reactors, this reactor type controls the system pressure using saturated coolant water in the steam dome at the top of the pressure vessel. Self-pressurization model is developed based on conservation of mass, volume, and energy by predicting the condensation that occurs in the steam dome and the flashing inside the chimney using the partial differential equation. A simple but functional model is adopted for the steam generator. The obtained results indicate that the variable measurement is consistent with design data and that this new model is able to predict the dynamics of the reactor in different situations. It is revealed that flashing and condensation power are in direct relation with the stability of the system pressure, without which pressure convergence cannot be established.

1. Introduction

Small (less than 300 MWe) and medium (300–700 MWe) reactors (SMRs) are being applied in contemporary power plants. In the late 70s, to fulfill the requirements of industrialized countries, it was common to apply larger reactor(s) in power plants. Gradual advances in this field made countries to develop small- and medium-sized reactors to be installed in different industries. In industrialized countries, nonelectrical applications of nuclear energy, such as desalination of seawater, have led to an application of a wide range of nuclear power plants [1].

SMRs have been and are being designed with respect to different parameters, such as modular technology, the pursuit of economics of series production, factory fabrication, and short construction times [2].

Studying different aspects of these types of reactors can assist scientists in this field in obtaining more knowledge. One important aspect is the stability analysis of SMRs equipped with self-pressurized and natural circulation features, which have many unknown elements.

There exist many different types of SMRs, categorized by their power range, safety system type, integral or nonintegral nature, coolant type, etc. One of the most popular types of SMRs is the self-pressurized natural circulation integral type, designed and manufactured in many countries [2].

Existing assessments indicate that in self-pressurized natural circulation integral-type SMRs, certain phenomena interact with one another, resulting in different dynamic results different from those of other reactors. Consequently, it is evident that combinations of complex effects make these reactors' behavior difficult to diagnose according to existing knowledge [3,4].

Zanocco et al. [5,6] assessed the density wave oscillation of a self-pressurized natural circulation integral-type SMR and determined the stability through linear and nonlinear approaches, in which the thermal-hydraulic code was improved for analyzing the stability. They revealed that in this type of reactor, oscillations are generated due to a counteraction between mass flow and buoyancy force in the chimney. The stability of the system is highly influenced by the steam-dome condensation power. Condensation in the steam zone, together with the reactor power, determines the dynamic state of the system. The feedback of the steam-dome

* *Corresponding author.*
E-mail address: m.esteki@eng.ui.ac.ir (M.H. Esteki).

https://doi.org/10.1016/j.net.2018.03.019

pressure is known as a stabilizing effect as long as it decreases the sensitivity of the buoyancy force.

Marcel et al. [3] assessed the phenomenology involved in the self-pressurized natural circulation in low thermo-dynamic quality of SMRs and determined the correlations between mass flow and core inlet enthalpy and their dependency on generated power, condensation power, and the location of flashing phenomenon in the chimney. Marcel et al. [4] assessed the stability of this type of reactor under both nominal and low pressure–low power conditions. They claim that the flashing phenomenon has an impact on the stability, and at transient conditions, the unstable region extends only from the core outlet up to the middle of the chimney. They found that, first, the condensation power has a great impact on the stability of the reactor and, then, that the reactor cannot be stable if condensation power is not considered in the equations.

Arda et al. [7,8] assessed the nonlinear dynamic modeling of the NuScale reactor. Their adopted model here is a combination of neutronics and thermal-hydraulics for the core, together with a single tube depiction with time-varying boundaries and three regions of subcooled, boiling, and superheated water for the helical-coil once-through steam generator (SG). Owing to the presence of a typical pressurizer, the model is developed based on the conservation of fluid mass, volume, and energy, where heater and spray are installed in the pressurizer.

Available studies run on this type of reactors have focused on density wave oscillation analysis based on the drift flux model, which can usually be applied in boiling water reactors (BWRs) [3–6]. These reactor types are categorized as something between pressurized water reactors and boiling water reactors [5]. A distinctive dynamic model with the capability of predicting the system behavior in the transient situation is essential. Thermal-hydraulic codes such as Relap5 simulate the behavior of the system through numerical methods [9], but they cannot generate distinct nonlinear differential equations for system analysis such as stability analysis or for controller design analysis, etc. A proper and functional model is thus required to constitute the basis for controller design according to one of the control models, such as transfer function, state space, direct Lyapunov theory, etc.

In this study, the subject reactor is a CAREM-25-like reactor, designed in Argentina. The reactor model is described in Section 2; a new dynamic model is proposed in Section 3; the methodology of this study is described in Section 4, and the results and conclusion are presented in Sections 5 and 6, respectively.

2. Reactor overview

This newly proposed reactor is a small modular reactor resembling a CAREM-25 reactor, designed and manufactured as an innovative nuclear power plant [2,10]. Some design features of the plant include an integrated primary cooling system, natural circulation, and self-pressurization of the primary system. There exists a high correlation among these features, which must be recognized in determining a good dynamic model of the system.

2.1. Natural circulation

The reactor pressure vessel (RPV) consists of the core, SGs, the whole primary coolant, and the absorber rods drive mechanisms, as shown in Fig. 1 [3]. The main parameters of this proposed reactor are enumerated in Table 1 [1–4,10].

Because the primary coolant flows subject to natural circulation in the RPV, coolant pump is eliminated here. The primary coolant is heated in the core and then enters the chimney, subject to natural condition in which convection and natural buoyancy generate enough force to give the fluid an upward orientation.

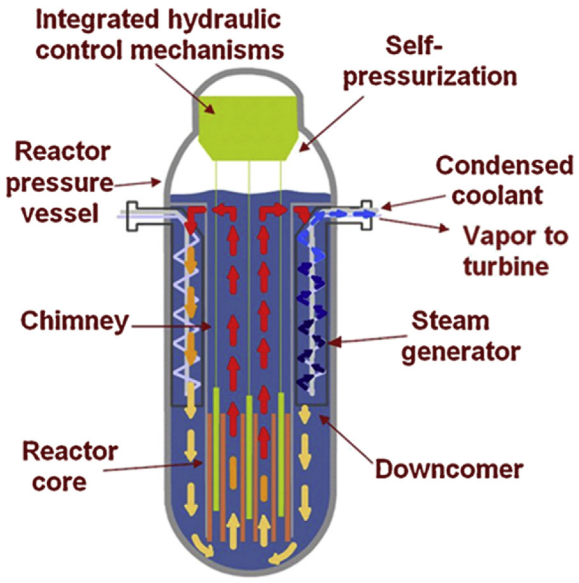

Fig. 1. Components of the reactor pressure vessel.

Table 1
Design features of the reactor.

Parameter	Value
Reactor thermal power	100 MWt
Inner diameter of RPV	3.16 m
Outer diameter of RPV	3.295 m
Height of RPV	11 m
Number of fuel assembly	61, hexagonal array
Number of fuel assembly with control rods	22
Number of fuel rods in each fuel assembly with control rods	90
Number of fuel rods in each fuel assembly without control rods	108
Number of absorber rods in each fuel assembly	18
Number of control rods in each fuel assembly	18
Active core height	1.4 m
Primary coolant pressure (light water)	12.25 MPa
Primary coolant mass flow rate in the normal power	410 (kg/s)
Core inlet temperature	557 K
Core outlet temperature	599 K
Feed water average temperature	518 K
Secondary fluid mass flow rate	48 (kg/s)
Number of steam generators	12
U-235 enrichment	<5%
Fuel cycle length	14 months

RPV, reactor pressure vessel.

After leaving the chimney, the coolant follows a downward path in the SG tubes, where the generated heat is transferred to the secondary side; next, it flows to the bottom of the core through the downcomer [1,2,10].

2.2. Self-pressurization

Unlike conventional PWRs, which are equipped with typical pressurizer to control the primary coolant pressure, this type of SMR controls coolant pressure through saturated water in the steam dome at the top of the RPV. This mechanism is called self-pressurization and is the result of liquid–vapor equilibrium [2].

There exist two distinct phenomena in RPV which have a direct link with self-pressurization: the flashing phenomenon and the condensation power.

Table 2
Nomenclature.

Nomenclature			
Q	Thermal power MW	x	Fluid quality
t	Time s	$\dot{m}$	Mass flow rate kg/s
Λ	Neutron generation time s		
C	Delayed neutron precursor	**Subscripts**	
β	Delayed neutron fraction	f	Fuel
λ	Decay constant 1/s	c	Coolant
ρ	Reactivity	sat	Saturation
T	Temperature K	se	Secondary side
α	Reactivity feedback coefficients 1/K	SG	Steam generator
m	Mass kg	CH	Chimney
c	Specific heat MJ/(kg K)	DC	Downcomer
V	Volume m^3	l	Liquid
A	Heat transfer area m^2	x	Quality
h	Enthalpy MJ/(kg K)	v	Vapor
E	Energy MW	su	Surge
K	Friction coefficient	ec	Exchange
R	Universal gas constant	r	Relative
g	Gravity acceleration m/s^2	0	Nominal
ρ	Density kg/m^3	P	Pressure
v	Specific volume m^3/kg	$cond$	Condensation
U	Heat transfer coefficient MW/(m^2 K)	tm	Tube metal

2.2.1. Flashing phenomenon

In this type of SMR, as the heated coolant exits the core, some vapor is generated in the chimney because of natural circulation. Both the hydrostatic pressure and the saturation temperature decrease depending on the chimney height, while the fluid temperature remains almost constant. At a given elevation of the chimney, when saturation temperature becomes equal to fluid temperature, vapor is generated. This phenomenon is called flashing [4].

The flashing phenomenon is crucial in fluid stability, especially in pressure control. In fact, the generated vapor here acts as a heater in the conventional pressurizer.

2.2.2. Condensation power

This power is the product of vapor condensation in the steam dome, a direct consequence of interaction between vapor and cold structures existing in the steam dome, similar to the control drive mechanism. This phenomenon is crucial for fluid stability as well [4]. The function of condensation power in the steam dome is similar to that of a spray in a conventional pressurizer.

3. System dynamic model

3.1. Reactor

The model of the reactor consists of a combination of neutronics and thermal-hydraulics equations. Neutronics equations are based on point kinetic theory, with three precursor groups. One precursor group is appropriate for low external reactivity but does not give a good response to high external reactivity [11]. Six precursor groups are appropriate for large reactors, and three groups are appropriate for SMRs, which are small. According to Hetrick [11], the Skinner–Cohen three groups model [12] is adequate to show neutronics behavior. There exists a small difference between the two models, the three and six groups. Simulation of the reactor core based on the six delayed neutron groups requires complicated calculations and more memory; therefore, the Skinner–Cohen model is a validated and practical model that is adopted in the reactor core simulation in this study.

$$\frac{dQ_r}{dt} = \frac{\delta\rho - \beta}{\Lambda} Q_r + \sum_{i=1}^{3} \frac{\beta_i}{\Lambda} C_{ri}, \; Q_r = \frac{Q}{Q_0} \tag{1}$$

$$\frac{dC_{ri}}{dt} = \lambda_i Q_r - \lambda_i C_{ri}, \; i = 1,2,3 \tag{2}$$

where Q_r is the reactor power density in relation to the initial equilibrium density (Q_0), C_{ri} is the group precursor relative density normalized with the initial equilibrium density, and $\delta\rho$ is the excess reactivity, expressed as Eq. (3):

$$\delta\rho = \delta\rho_{ex} + \alpha_f \delta T_f + \alpha_c \delta T_c + \alpha_P \delta P \tag{3}$$

where $\delta\rho_{ex}$ is the external reactivity from the control rods, δT_f is the deviation from the former state for fuel temperature, δT_c is the deviation from the former state for coolant temperature, and δP is the deviation from the former state for coolant pressure.

The thermal-hydraulics model of the reactor core is expressed as follows, provided these assumptions hold true:

1. The heat flux is uniform in the axial direction
2. Primary coolant is considered to be well stirred
3. The fuel-to-coolant heat transfer coefficient is a function of mass flow rate
4. Only single-phase natural circulation is considered
5. The Boussinesq approximation is valid.

$$T_c = \frac{T_{ci} + T_{co}}{2} \tag{4}$$

$$m_f c_f \frac{dT_f}{dt} = f_f Q_r Q_0 - U_c A_f \left(T_f - T_c\right) \tag{5}$$

$$m_c c_c \frac{dT_c}{dt} = \left(1 - f_f\right) Q_r Q_0 + U_c A_f \left(T_f - T_c\right) - \dot{m}_c \, c_c (T_{co} - T_{ci}) \tag{6}$$

where f_f is the fraction of the total power directly deposited in the fuel, $T_{ci}$is the core inlet temperature, T_{co} is the core outlet temperature, and $\dot{m}_c$is the mass flow rate, calculated by equating the buoyancy force and friction losses [3]:

$$\dot{m}_c = \sqrt[3]{\frac{2\rho_{core}^2 A_{eq}^2 \beta_T g Q_r Q_0 \Delta L}{K \overline{C}_{P,core}}} \tag{7}$$

where ρ_{core} is the average coolant density of the core, A_{eq} is the equal cross section, ΔL is the direct distance from the center of the core to the center of the SG, β_T is the thermal expansion coefficient, and $\overline{C}_{P,core}$ is the specific heat average in the core.

3.2. Chimney and downcomer

There is no heat source in either the chimney or the downcomer; consequently, the dynamic equations for these sections are treated as first-order lags due to natural circulation, expressed as follows:

$$\frac{dT_{CH}}{dt} = \frac{1}{\tau_{CH}} (T_{co} - T_{CH}) \tag{8}$$

$$\frac{dT_{DC}}{dt} = \frac{1}{\tau_{DC}} (T_{SGo} - T_{DC}) \tag{9}$$

where τ_{CH} and τ_{DC} are the residence times ($\tau = \frac{m}{\dot{m}}$)and T_{SGo} is the SG outlet temperature. This model is validated in different studies, such as in those of Arda et al. [7,8].

3.3. Steam generator

In this study, the SG model is simple but more functional in relation to the models adopted in previous studies, in which the final forms of mass and energy balance equations are applied for all secondary side regions (subcooled, two-phase, and superheat), and the focus is on feed water fluid. The focus of this newly proposed model is on primary fluid, which is appropriate for stability analysis applications, for nonlinear stability specifically.

The model of the SG applied here is that of Ansarifar [13], as follows, provided that these assumptions hold true:

1. The secondary side is at saturation condition
2. Heat transfer coefficient is a function of mass flow rate on the fluid motion path
3. There is no carry-under of bubbles to the SG.

The average primary coolant temperature is

$$T_{SG} = \frac{T_{SGi} + T_{SGo}}{2} \tag{10}$$

where T_{SGi} is the primary inlet temperature in the SG.

The energy conservation equation for the primary circuit is expressed as follows:

$$m_{SG} c_{SG} \frac{dT_{SG}}{dt} = \dot{m}_{SG}\, c_{SG}(T_{SGi} - T_{SGo}) - U_{SG} A_{SG}(T_{SG} - T_{tm}) \tag{11}$$

Heat transfers from the primary side to the tubes and from the tubes to the secondary side. Here, the energy conservation equation for the tubes is expressed as follows:

$$\rho_{tm} V_{tm} c_{tm} \frac{dT_{tm}}{dt} = U_{SG} A_{SG}(T_{SG} - T_{tm}) - U_{se} A_{se}(T_{tm} - T_{sat}) \tag{12}$$

It is notable that because the SG is a U-tube SG in the Ansarifar model [13], the correlations for heat transfer on both sides are different from those of the semihelical SG applied in this reactor. In this study, the heat transfer coefficient for the primary fluid is calculated through the correlation for a bank of tubes, given by Incropera [14].

$$Nu = B\mathrm{Re}^{b}\mathrm{Pr}^{0.36}\left(\frac{\mathrm{Pr}}{\mathrm{Pr}_s}\right)^{0.25} \tag{13}$$

where Nu is the Nusselt number, parameters B and b are determined according to the configuration, Pr is the Prandtl number, and Pr_s is the Prandtl number at the surface conditions. For the surface heat transfer coefficient of the secondary fluid, the Dittus-Boelter correlation [15] is applied, as follows:

$$Nu = 0.023\mathrm{Re}^{0.85}\mathrm{Pr}^{0.4}\left(\frac{d_o}{d_c}\right)^{0.1} \tag{14}$$

where Re is the Reynolds number, d_o is the outer diameter of the tube metal, and d_c is the coil diameter.

3.4. Steam dome

Unlike conventional PWRs, which have typical pressurizers to control primary fluid pressure, this reactor controls system pressure using saturated water in the steam dome at the top of the RPV.

Because of the impact of condensation power and the flashing phenomenon on pressure, a new pressure partial differential equation (PDE) must be introduced; thus, the dynamic model for the steam dome is determined based on the following assumptions:

1. Total volume of fluid in the steam dome is constant
2. Fluid in the steam dome is always in saturation state
3. Condensation power only occurs in the steam dome.

This model is based on the mass and energy conservation equations. The flashing and condensation model was validated for this reactor in previous works [3,4,6].

Volume balance equation for the steam dome model is presented as follows:

$$V_T = V_l + V_v \tag{15}$$

where V_T is the total volume of the steam dome, that is,

$$\frac{dV_T}{dt} = 0 \Rightarrow \frac{dV_l}{dt} = -\frac{dV_v}{dt} \tag{16}$$

The mass and energy balance equations are presented as follows:

$$\frac{dm_l}{dt} = \dot{m}_{su} - \dot{m}_{ec} \tag{17}$$

$$\frac{dm_v}{dt} = \dot{m}_{ec} + \dot{m}_x \tag{18}$$

$$\frac{dE_l}{dt} = \dot{m}_{su}\, h - \dot{m}_{ec}\, h_g - P\frac{dV_l}{dt} \tag{19}$$

$$\frac{dE_v}{dt} = \dot{m}_{ec}\, h_g - Q_{cond} - P\frac{dV_v}{dt} + \dot{m}_x\, h_g \tag{20}$$

where $\dot{m}_x$ is the vapor in the chimney that moves upward and is added to the steam regime; h is the average chimney enthalpy if $\dot{m}_{su} > 0$, and otherwise $h$is the liquid enthalpy; h_g is the steam enthalpy; and Q_{cond} is the condensation power.

By expanding Eqs. (19) and (20), which are then substituted by Eq. (16), Eq. (23) yields

$$m_l \frac{\partial h_f}{\partial t} + P\frac{dV_L}{dt} = \dot{m}_{su}\left(h - h_f\right) - \dot{m}_{ec}\, h_{fg} \tag{21}$$

$$m_v \frac{\partial h_g}{\partial t} = -Q_{cond} - P\frac{dV_v}{dt} \tag{22}$$

$$\left(m_l \frac{\partial h_f}{\partial P} + m_v \frac{\partial h_g}{\partial P}\right)\frac{dP}{dt} = \dot{m}_{su}\left(h - h_f\right) - \dot{m}_{ec}\, h_{fg} - Q_{cond} \tag{23}$$

where h_f is the fluid enthalpy, $h_{fg} = h_g - h_f$.

By assuming that steam follows the ideal gas law and by applying Eq. (24) and a combination of Eqs. (16) and (18), Eq. (25) is the result:

$$PV_v = m_v R T_{sat} \tag{24}$$

$$\dot{m}_{ec} + \dot{m}_x = \frac{1}{A}\frac{dP}{dt} - \frac{B}{A}\frac{dm_l}{dt} \tag{25}$$

where A&$B$are calculated through Eqs. (26 and 27):

$$A = \frac{RT_{sat}}{V_v - Rm_v \frac{\partial T_{sat}}{\partial P} - Pm_l \frac{\partial v_l}{\partial P}} \tag{26}$$

$$B = \frac{Pv_l}{V_v - Rm_v \frac{\partial T_{sat}}{\partial P} - Pm_l \frac{\partial v_l}{\partial P}} \tag{27}$$

Finally, the PDE for pressure is calculated by combining Eqs. (17, 23 and 25), as follows:

$$\left[m_l \frac{\partial h_f}{\partial P} + m_v \frac{\partial h_g}{\partial P} + \frac{h_{fg}}{A-B}\right] \frac{dP}{dt} = \dot{m}_{su} \left(h - h_f + \frac{B}{A-B} h_{fg}\right) - Q_{cond} + \frac{Ah_{fg}}{A-B} \dot{m}_x \tag{28}$$

The value of $\delta\dot{m}_{su}$ is calculated using Eq. (29) [16], and Q_{cond} is determined using Eq. (30) [3], as follows:

$$\delta\dot{m}_{su} = -\sum_{i=1}^{n} V_i \vartheta_i \frac{d\delta T_i}{dt} \tag{29}$$

$$Q_{cond} = \dot{m}(h_{co} - h_{sat,o}) \tag{30}$$

where ϑ is the density gradient with respect to temperature, index i refers to the core, SG, chimney, and downcomer, h_{co} is the core outlet enthalpy, and $h_{sat,o}$ is the chimney outlet saturation enthalpy.

The first step in calculating $\dot{m}_x$ is to determine the average quality of flow at the chimney outlet. The beginning point of flashing y in the chimney must be measured to calculate the quality, as follows [3]:

$$y = \frac{Q_{cond}}{\dot{m}} \frac{1}{\rho g \frac{\delta h_{sat}}{\delta P}\Big|_{p=p_{sys}}} \tag{31}$$

The liquid quality at the chimney outlet is measured using Eq. (32) [17]:

$$x = \frac{(h_{co} - h_{sat,o})}{h_{fg}} \tag{32}$$

Consequently, $\dot{m}_x$ is obtained by multiplying the average quality ($\frac{xy}{2}$) of the chimney by the flow rate:

$$\dot{m}_x = \frac{xy}{2} \dot{m} \tag{33}$$

4. Methodology

This model is applied to predict system behavior in the operating range and transient states throughout the reactor cycle length. The objective of this study is to propose a new dynamic model capable of predicting system behavior in normal condition or usual transient condition. This kind of reactor has passive shutdown and emergency injection systems with crucial effects on the system in accident conditions [1,10]. It is important that the model of the failure scenario of the reactor include shutdown and emergency injection dynamics, something beyond the scope of this study.

According to the PDEs, given here, the state space model is appropriate for linear stability analysis. In this model, variables for the system are represented as Q_r,C_1,C_2, C_3, T_f, T_c, T_{CH}, T_{DC}, T_{SG}, T_{tm}, and P.

The safety system in this reactor is passive, and there is no boron in the reactor [1,2,10]. There is no heater or spray in the system because of self-pressurization. The control rods are the only means to change the steady-state situation of the primary coolant. The dynamic model is appropriate for steady-state or usual transient conditions, which are controlled only by the control rods. The input variable is the external reactivity, represented as ($\delta\rho_{ex}$).

5. Results

This reactor model is implemented in MATLAB/Simulink [18] to yield the steady-state and dynamic conditions. The block diagram of this model is shown in Fig. 2, where the flow rate and outlet temperature of each section are applied for another section. The average temperature of each section is applied to calculate the pressure in the steam dome. The RELAP5/MOD3.3 code [9] is applied to validate the simulation, and the results of this model are compared with those of the RELAP5 code. RELAP5 is a best-estimate code developed by the Idaho National Engineering Laboratory and is well validated. It is widely used in nuclear power plant simulations and analyses [19].

The nodalization of the RPV in RELAP5 code is shown in Fig. 3. Coolant channels in the reactor core are divided into two parts, one hot channel (040P) and one normal channel (030P). Under natural circulation, the primary coolant flows through the chimney (035P) into the SG (002A and 003P), releasing heat, and then flows into the downcomer (004A). The secondary fluid flows upward with a 48-kg/s mass flow rate (151A) and receives heat from the primary coolant. The space at the pressure vessel top is used as a self-pressurizer (27B, 28B, 46B and 49B).

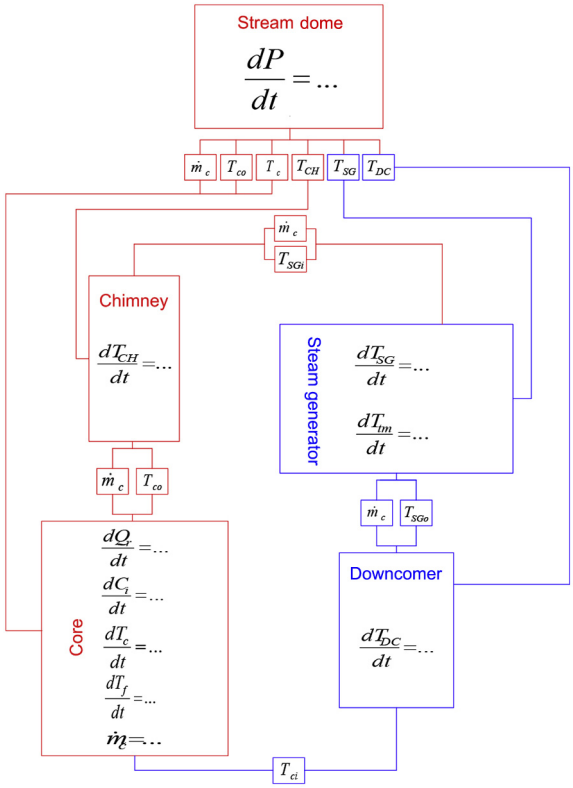

Fig. 2. Schematic block diagram of the simulated model.

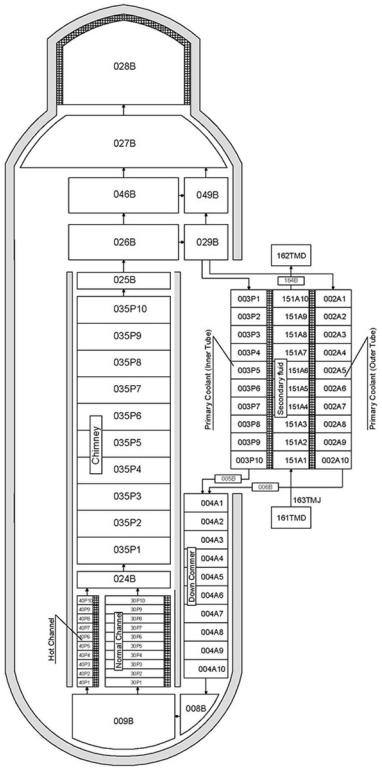

Fig. 3. The RELAP5 nodalization of the reactor pressure vessel.

5.1. Steady state

The outcomes of reactor power, system pressure, inlet and outlet temperature, and mass flow rate, in steady-state condition at nominal power, determined using MATLAB/Simulink, Relap5, and design data, are shown in Table 3. A comparison of these results indicates that there exists a consistency among them. The obtained results verify the applied dynamic model. Steam-dome pressure profile in three cases of without flashing phenomenon, without condensation power, and with both of them are shown in Figs. 4–6. It is obvious that without either of these two phenomena, convergence of pressure cannot be guaranteed.

5.2. Dynamic condition

In a reactor of this type, power is controlled by the control rods. The movements of the control rods increase or decrease the reactor reactivity, as expressed by the external reactivity. Here, in the first case, a step reactivity, $3.5 \times 10^{-4}\frac{\Delta k}{k}$ at t = 20s, is applied to the system, as shown in Fig. 7. The second case is an external ramp reactivity applied to the system for 300 s, as shown in Fig. 16.

Table 3
System parameters at steady-state condition.

Parameter	Value		
	Design data	MATLAB	Relap5
Reactor thermal power	100 MWt	100 MWt	100 MWt
Primary coolant pressure (light water)	12.25 MPa	12.248 MPa	12.24 MPa
Primary coolant mass flow rate in the normal power	410 kg/s	409.9 kg/s	410.21 kg/s
Core inlet temperature	557 *K*	557.02 *K*	556.8 *K*
Core outlet temperature	599 *K*	599 *K*	598.8 *K*

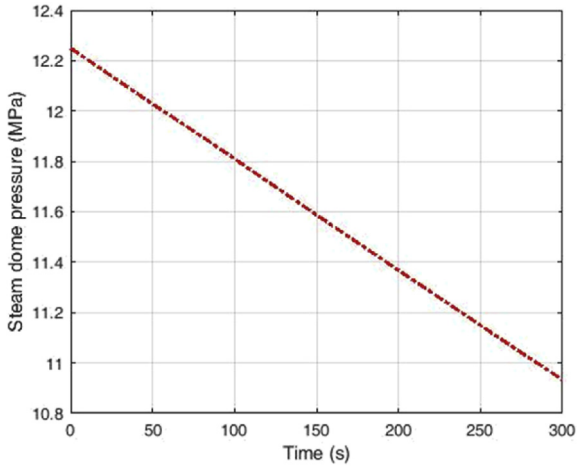

Fig. 4. Steam dome pressure profile without flashing phenomenon in steady-state condition.

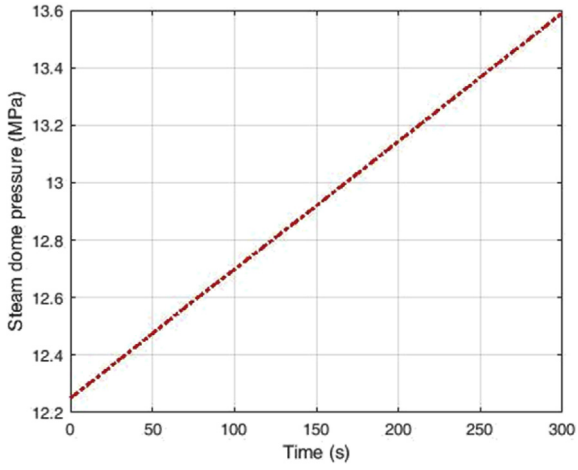

Fig. 5. Steam dome pressure profile without condensation power in steady-state condition.

As can be observed in Figs. 7–15, for the first case, variations of the variables in this model and in the RELAP5 model are almost the same, and the difference between them is mainly due to the steady-state condition, the time before the transient condition.

The core-normalized power profile is shown in Fig. 8. Owing to the increase in ($\delta\rho_{ex}$), at first, a prompt jump occurs in the power, which reaches about 105 MW and then decreases, though the ultimate power is still slightly more than that before.

The steam dome pressure profile is shown in Fig. 9. An increase in the core power leads to a disturbance in the pressure; finally, the interaction between flashing and condensation power stabilizes the pressure.

The coolant mass flow rate profile is shown in Fig. 10. As expressed in Eq. (7), $\dot{m} \propto Q_r^{1/3}$. Change in coolant mass flow rate is proportional to core-normalized power. At first, by increasing the core power, the mass flow rate increases to 417.2 kg/s, but then it decreases due to a decrease in the power.

The core fuel and the inlet and outlet primary coolant temperature profiles, showing how the increased power generation causes the fuel temperature to rise and transfer more heat from the fuel to the coolant, are shown in Figs. 11–13. This external reactivity causes

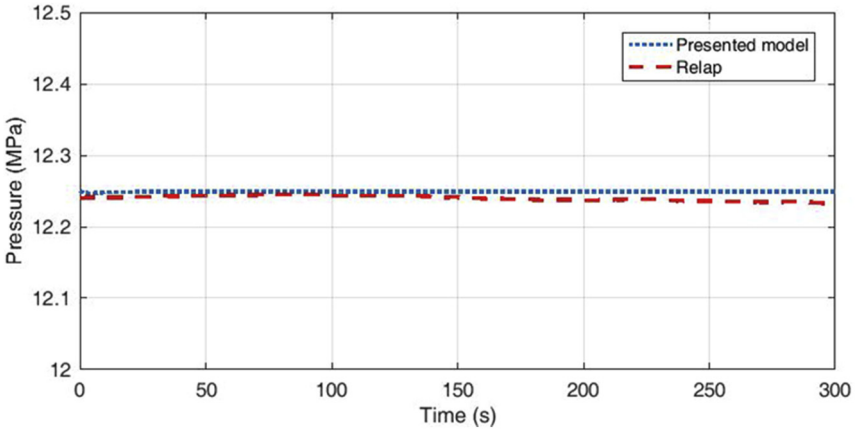

Fig. 6. Steam dome pressure profile in steady-state condition.

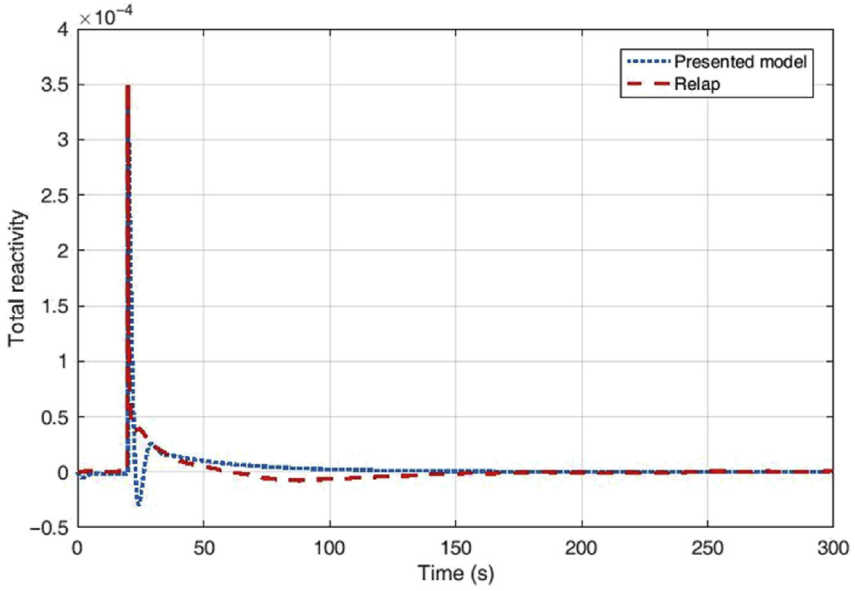

Fig. 7. System reactivity response to a step increase in the input variable.

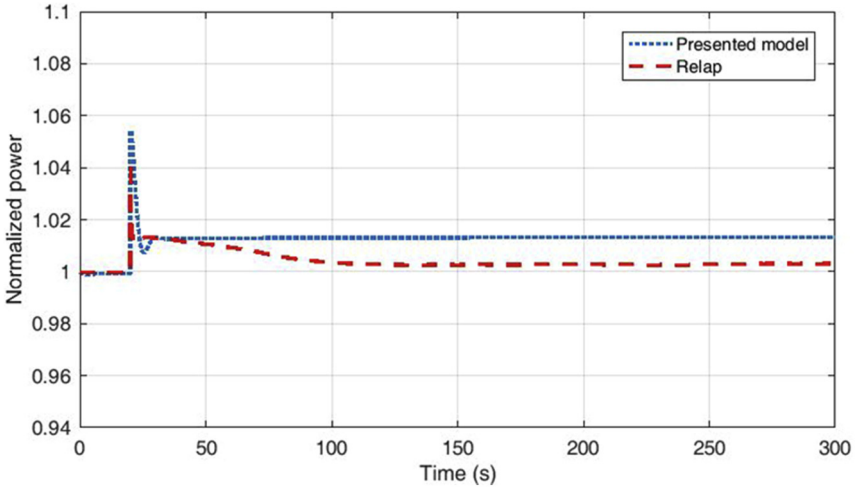

Fig. 8. Core-normalized power response to a step increase in the input variable.

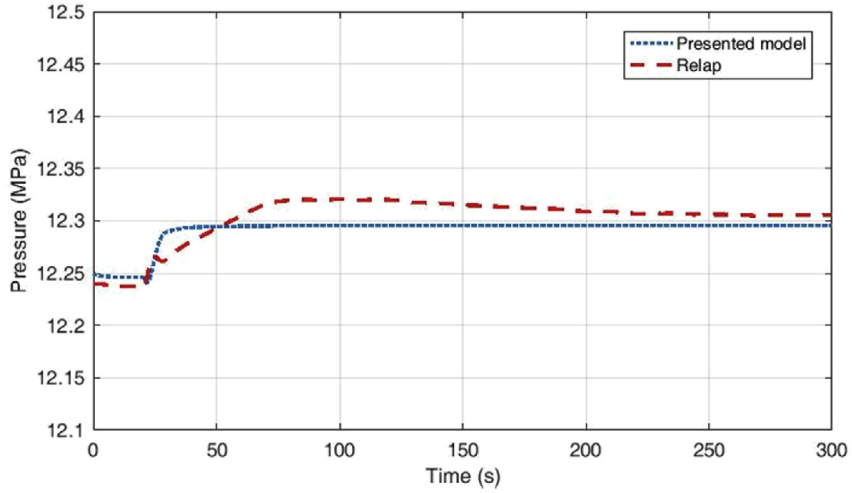

Fig. 9. System pressure response to a step increase in the input variable.

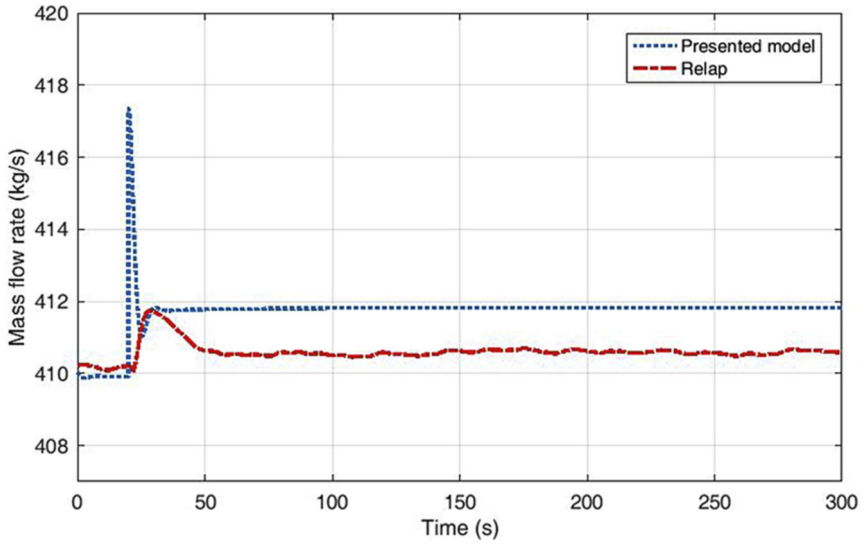

Fig. 10. Coolant mass flow rate response to a step increase in the input variable.

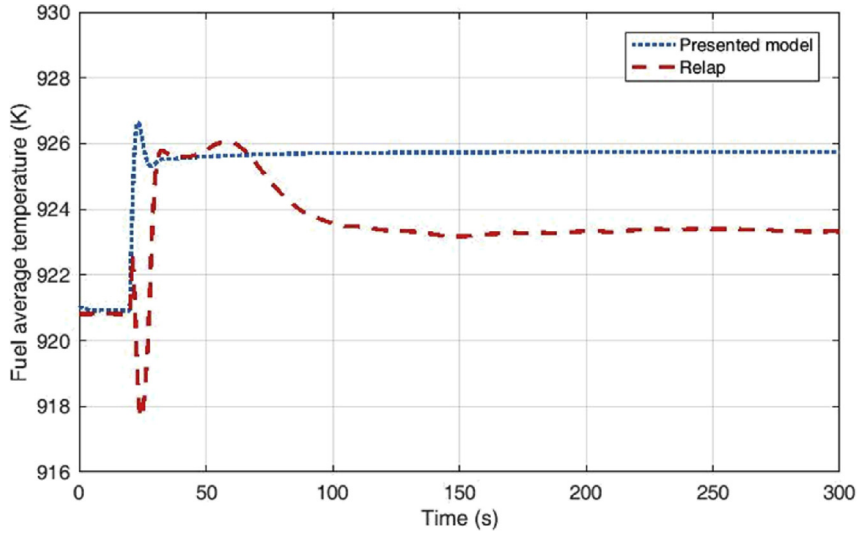

Fig. 11. Core fuel average temperature response to a step increase in the input variable.

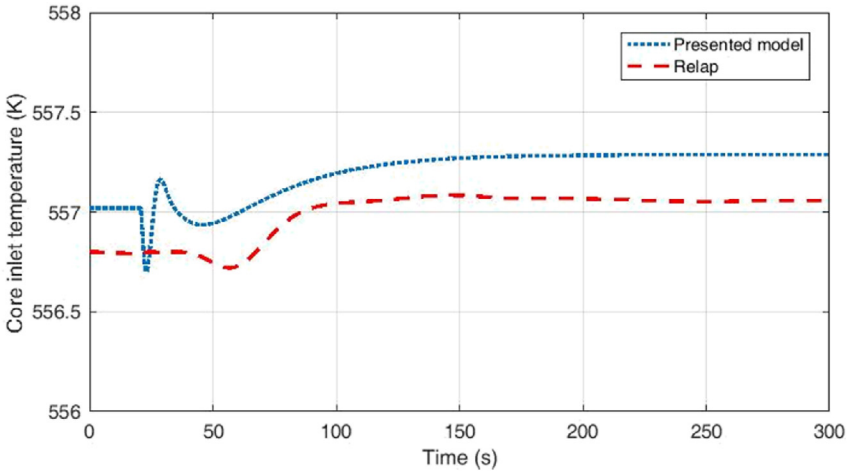

Fig. 12. Core primary coolant inlet temperature response to a step increase in the input variable.

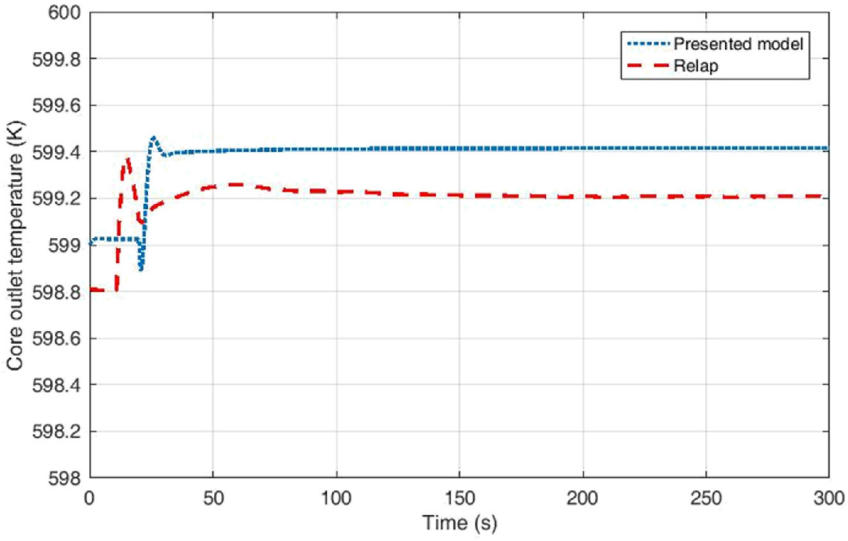

Fig. 13. Core primary coolant outlet temperature response to a step increase in the input variable.

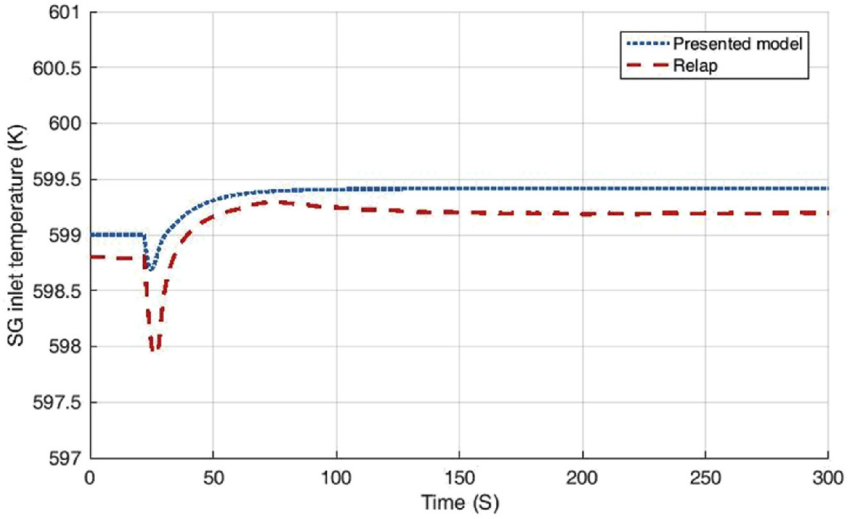

Fig. 14. SG primary coolant inlet temperature response to a step increase in the input variable.

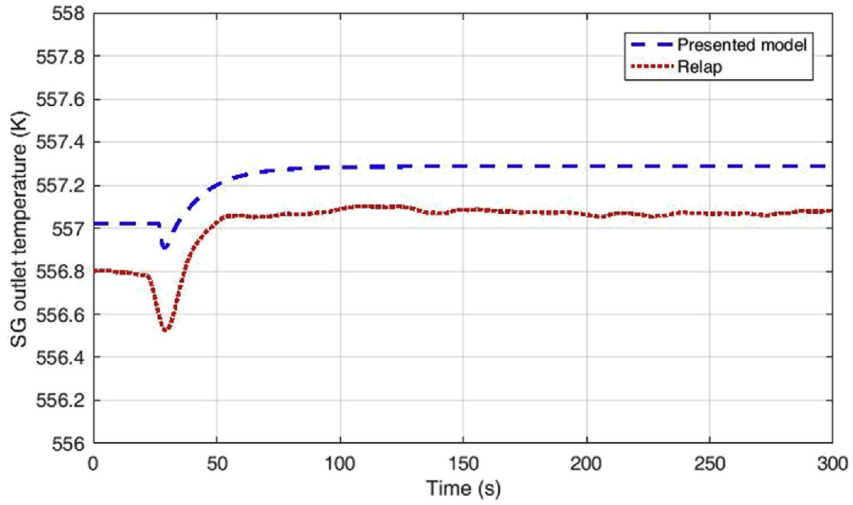

Fig. 15. SG primary coolant outlet temperature response to a step increase in the input variable.

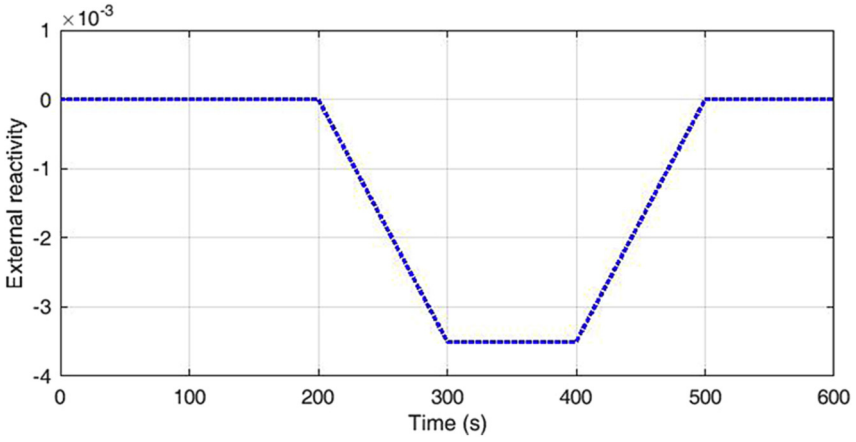

Fig. 16. External ramp reactivity.

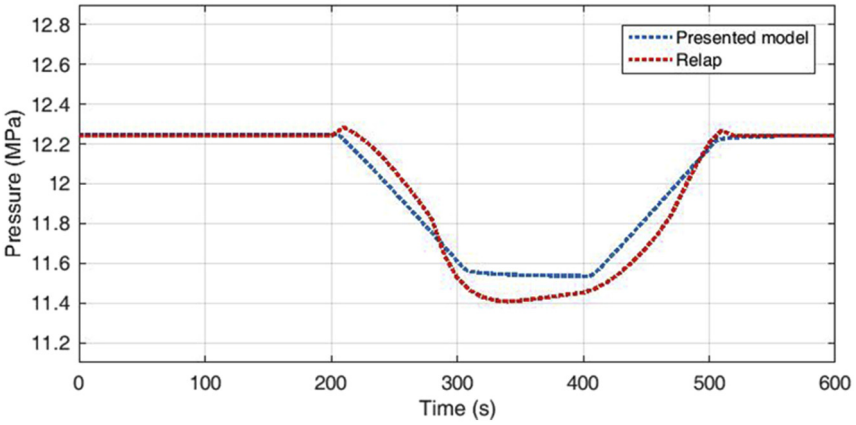

Fig. 17. System pressure response to an external ramp reactivity.

an increase of about 4.5*K*in the fuel temperature and a slight increase in the primary coolant temperature.

The SG inlet and outlet coolant temperature profiles, in which the increased power generation can be seen to cause the core coolant temperature to increase and in which the SG temperature can be seen to increase with a phase lag because of the chimney model, are shown in Figs. 14 and 15. This phase lag is clearly observable in Figs. 13–15.

For the second case, the validity of the pressure model presented in Eq. (28) is measured by external ramp reactivity. External reactivity is applied to the system during a period of 300 s, as can be seen in Fig. 16. The steam dome pressure profile is shown in Fig. 17. As can be observed in this figure, the variations of the pressure in this model and in the RELAP5 model are almost the same.

Consequently, comparing the results of the presented model with those of the RELAP5 shows that the presented dynamic model can show the behavior of the system in the medium range of transient conditions. Other transient conditions, such as failure scenarios and the effects of poisons, can be added to this model in further studies.

6. Conclusion

A new self-pressurized dynamic model of a small reactor is proposed based on the conservation of mass, volume, and energy and by predicting the condensation power and flashing phenomenon. Compared with the available studies, the SG model here is simpler, with more functionality for stability analysis. The results obtained for steady-state and dynamic conditions indicate that the measures of the variables are consistent with design data and that this newly proposed model is able to predict the dynamics of the reactor. Moreover, the flashing phenomenon and the condensation power are found to be directly connected with the self-pressurization of the reactor, without which the reactor pressure cannot be stabilized.

The proposed dynamic model is able to predict system behavior in the steady-state and medium range of transient conditions. In further studies, by adding dynamic equations for poisons, passive shutdown, and emergency injection systems, other transients such as failure scenarios and the effects of poisons can be considered in this model. This dynamic model can be adopted in linear and nonlinear stability analysis and for designing pressure control system(s) in future study.

Conflicts of interest

This study is as part of the requirement for Mr. Ali Pharsoon Pilehvar's PhD thesis in the University of Isfahan and the authors (student and his supervisors) hereby declare there is no conflict of interest between them in this research.

Appendix A. Supplementary data

Supplementary data related to this article can be found at https://doi.org/10.1016/j.net.2018.03.019.

References

[1] D. Delmastro, An advanced integrated PWR, in: International Seminar Held in Cairo, Egypt, 2002, pp. 27–31.
[2] International Atomic Energy Agency (IAEA), Status of Small and Medium Sized Reactor Designs, 2012, pp. 4–5. https://aris.iaea.org/Publications/smr-status-sep-2012.pdf.
[3] C.P. Marcel, F.M. Acuna, P.G. Zanocco, D.F. Delmastro, Stability of self-pressurized, natural circulation, low thermo-dynamic quality, nuclear reactors: the stability performance of the CAREM-25 reactor, Nucl. Eng. Des. 265 (2013) 232–243.
[4] C.P. Marcel, H.F. Furci, D.F. Delmastro, V.P. Masson, Phenomenology involved in self-pressurized, natural circulation, low thermo-dynamic quality, nuclear reactors: the thermal–hydraulics of the CAREM-25 reactor, Nucl. Eng. Des. 254 (2013) 218–227.
[5] P. Zanocco, D. Delmastro, M. Gimenez, Linear and nonlinear stability analysis of a self-pressurized, natural circulation, integral reactor, in: ICONE12, International Conference on Nuclear Engineering, 2004. Washington, DC.
[6] P. Zanocco, M. Gimenez, D. Delmastro, Modeling aspects in linear stability analysis of a self-pressurized natural circulation integral reactor, Nucl. Eng. Des. 231 (2004) 283–301.
[7] S.E. Arda, K.E. Holbert, Nonlinear dynamic modeling and simulation of a passively cooled small modular reactor, Prog. Nucl. Energy 91 (2016) 116–131.
[8] S.E. Arda, K.E. Holbert, A dynamic model of a passively cooled small modular reactor for controller design purposes, Nucl. Eng. Des. 289 (2015) 218–230.
[9] Inc, RELAP5/MOD3.3 Code Manual, Volume II, Appendix A, Input Requirements, 2002.
[10] International Atomic Energy Agency (IAEA), Status of Innovative Small and Medium Sized Reactor Designs, 2006. http://pub.iaea.org/MTCD/publications/PDF/te-1485-web.pdf.
[11] D.L. Hetrick, Dynamics of Nuclear Reactor, The University of Chicago Press, 1971.
[12] R.E. Skinner, E.R. Cohen, Reduced delayed neutron group representation, Nucl. Sci. Eng. (1959) 5–291.
[13] G.R. Ansarifar, Control of the nuclear steam generators using adaptive dynamic sliding mode method based on the nonlinear model, Ann. Nucl. Energy 88 (2016) 280–300.
[14] F.P. Incropera, Fundamentals of Heat and Mass Transfer, John Wiley & Sons, 2011.
[15] L. Zhao, L. Guo, B. Bai, Y. Hou, X. Zhang, Convective boiling heat transfer and two-phase flow characteristics inside a small horizontal helically coiled tubing once-through steam generator, Int. J. Heat Mass Transf 46 (25) (2003) 4779–4788.
[16] Electric Power Research Institute (EPRI), Pressurized Water Reactor Modeling for Long-term Power System Dynamics Simulation, 1983.
[17] R.E. Sonntag, C. Borgnakke, G.J. Van Wylen, Fundamental of Thermodynamic, John Wiley & Sons Press, 2003.
[18] Mathworks, SIMULINK Dynamic System Simulation Language User's Guide, 2016.
[19] Z.L. Wang, W.X. Tian, G.H. Su, S.Z. Qiu, L. Zhao, Q.L. Zuo, Y.W. Wu, D.L. Zhang, Development of a thermal hydraulic code for an integral reactor, Prog. Nucl. Energy 68 (2013) 31–42.